

Functional Localized High-Concentration Ether-Based Electrolyte for Stabilizing High-Voltage Lithium-Metal Battery

Shuangshuang Lin, Haiming Hua, Zhisen Li, and Jinbao Zhao*



Cite This: <https://dx.doi.org/10.1021/acsami.0c07904>



Read Online

ACCESS |



Metrics & More



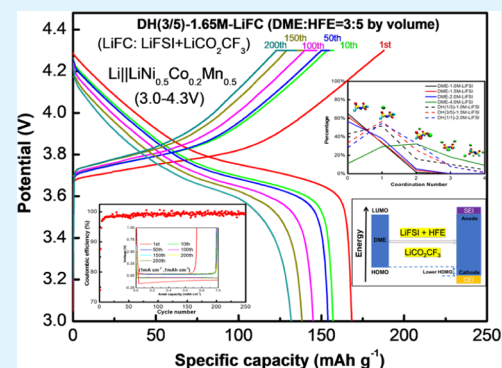
Article Recommendations



Supporting Information

ABSTRACT: Localized high-concentration electrolytes have attracted much attention of researchers due to their low viscosity, low cost, and relatively higher electrochemical performance than their low-concentration counterparts. In our work, 1.5 M (mol L⁻¹) locally concentrated ether-based electrolyte has been obtained by adding 1,1,2,2-tetrafluoroethyl-2,2,3,3-tetrafluoropropyl ether (HFE) into a 4 M LiFSI concentrated dimethoxyethane (DME)-based electrolyte. The optimal ratio is determined by density functional theory (DFT) calculation and experimental combination, and finally, DH(3/5)-1.5M-LiFSI (DME/HFE = 3:5 by volume) is obtained. The electrolyte not only has relatively good physical properties such as low viscosity and high conductivity but also shows decent electrochemical performance. Li||Cu half-cells can maintain a coulombic efficiency of no less than 99% after circulating for 250 cycles under the condition of 1 mA cm⁻² current density and 1 mAh cm⁻² lithium deposition for each cycle, and the stable battery polarization voltage was about 50 mV. Furthermore, 0.15 M lithium trifluoromethyl acetate (LiCO₂CF₃) has been added as an additive to enhance the oxidation stability. The new electrolyte DH(3/5)-1.65M-LiFC (LiFC/LiFSI + LiCO₂CF₃) makes Li||NCM523 batteries maintain about 83% capacity after cycling for 250 times with a 0.5 C charge current density and a 1 C discharge current density of 160 mAh g⁻¹ when charged to 4.3 V. Furthermore, this new additive has a little negative effect on the Li||Cu half-cell performance under the same condition as before, indicating this new type of localized high-concentration DME-based electrolyte benefits both high-voltage cathode and lithium-metal anode.

KEYWORDS: ether-based electrolyte, localized high concentration, high voltage, lithium-metal battery, LiCO₂CF₃ additive



1. INTRODUCTION

It is well known that lithium metal¹ has an extremely low electrode voltage of -3.04 V and a superhigh theoretical specific capacity of 3860 mAh g⁻¹, so it is considered as the “holy grail” of energy batteries. However, lithium metal is easy to pulverize during the cycle, thus reducing the battery stability. Moreover, dendrite growth may even cause safety issues due to short circuit, which also greatly limits subsequent applications of the battery. Nowadays, with the continuous pursuit of high-energy-density²⁻⁸ storage devices, researchers have devoted great interest in the research of lithium-metal batteries,⁹⁻²⁴ and using high-concentration electrolytes (HCEs)^{19,25-29} to inhibit lithium dendrite³⁰ has also become a popular choice. In 2008, Jeong et al.³¹ reported that PC(propylene carbonate)-based high-concentration electrolytes can effectively inhibit lithium dendrite formation on Li metal anode. Suo et al.³² and Qian et al.,²⁹ respectively, reported in 2013 and 2015 that high-concentration electrolytes can provide good reversible performance of lithium-metal batteries and greatly inhibit the dissolution of lithium polysulfide compounds in Li-S batteries. In 2013, Matsumoto et al.³³ reported that concentrated electrolytes can effectively suppress Al collector corrosion. Yoon et al.³⁴ reported 3.27 M

LiBETI (lithium pentafluoroethanesulfonimide)/PC as a high-concentration electrolyte and found that it can form a thin solid electrolyte interface (SEI) layer on the surface of Li metal anode and refrain dendrite growth. In 2018, Fan et al.²⁷ used a 10 M lithium bis(fluorosulfonyl)imide (LiFSI)/dimethyl carbonate (DMC) concentrated electrolyte to not only make the Li||Cu half-cells show excellent performance but also stabilize Li||LiNi_{0.6}Co_{0.2}Mn_{0.2} batteries at a high voltage of 4.6 V. Nevertheless, there are also many problems with high-concentration electrolytes: (1) The ionic conductivity is low, which influences the battery rate performance; (2) lithium is easy to precipitate at a low temperature, resulting in poor low-temperature performance; (3) viscosity is quite high, and hence it is difficult to wet the separator and in turn degrades battery performance; (4) the cost is very high, thereby making their large-scale commercial applications difficult. At present,

Received: April 29, 2020

Accepted: June 29, 2020

Published: June 29, 2020



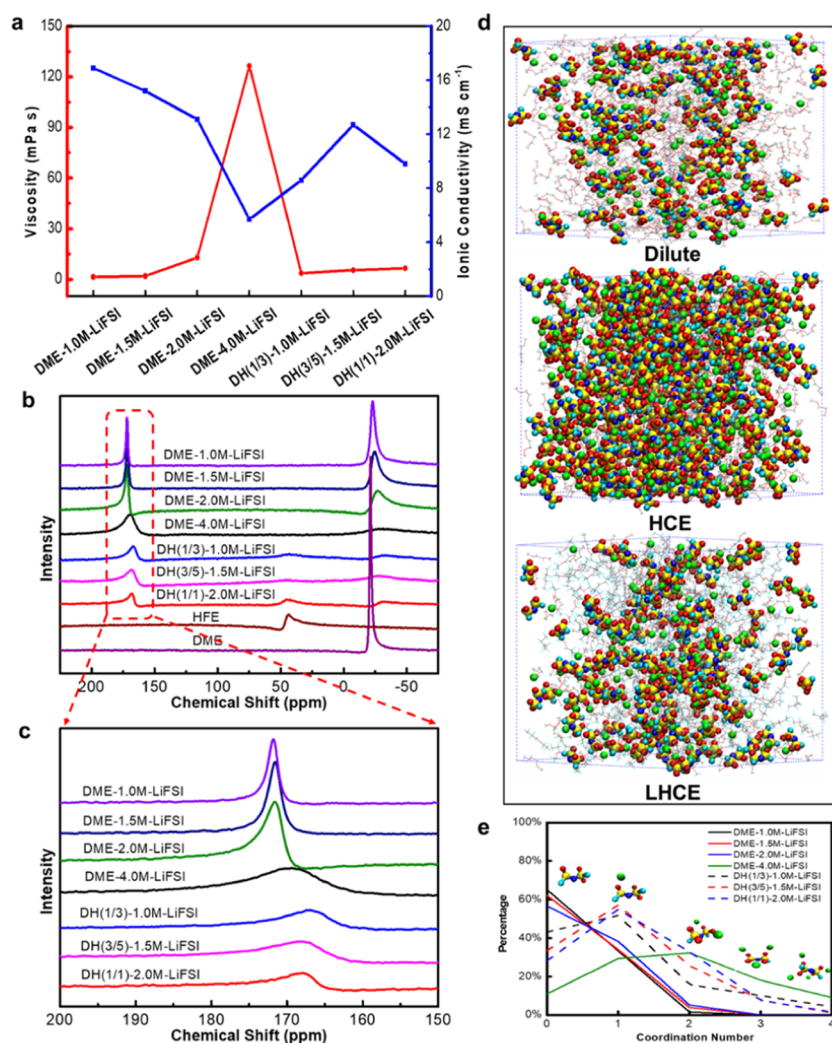


Figure 1. (a) Ionic conductivity and viscosity and (b) ¹⁷O NMR spectra. (c) Partial enlargement of (b) of different electrolytes at room temperature; (d) Theoretical simulation results of coordination between solvents and lithium salts in three concentrations including dilute solution: (DME-1.5M-LiFSI), HCE (DME-4.0M-LiFSI), and LHCE (DH(3/5)-1.5M-LiFSI). (e) Ionic association conditions of seven kinds of different electrolytes. (Coordination number is the number of Li⁺ cations coordinating with FSI⁻ anions).

inert solvents that have low viscosity and high electrochemical stability and do not undergo solvation with Li⁺ can be used to solve the above problems. Doi et al.³⁵ tried to add a variety of fluoroalkyl ethers into a 3.75 mol kg⁻¹ lithium tetrafluoroborate (LiBF₄)/PC electrolyte to decrease the viscosity. And the localized high-concentration electrolyte maintained a decent layer-forming performance as the low-concentration counterpart so that the batteries still had excellent oxidation stability under high-voltage condition. Ren et al.³⁶ added HFE to the LiFSI/ethylmethyl sulfone (EMS) concentrated electrolyte to obtain a localized high-concentration sulfone electrolyte so as to make the battery system achieve excellent performance at 4.9 V. Zheng et al.³⁷ had chosen 1*H*,1*H*,5*H*-octafluoramyl-1,1,2,2-tetrafluoroethyl ether as a co-solvent of the LiFSI/dimethoxyethane (DME) high-concentration electrolyte system, which promoted Li-S battery performance. Inspired by this, we also attempted to achieve a locally concentrated electrolyte^{38,39} to optimize electrolyte performance.

In our work, we chose the 4 M LiFSI DME-based high-concentration ether electrolyte²⁹ as a basis and added the commonly used diluent HFE to prepare a localized high-concentration DME-based electrolyte DH(3/5)-1.5M-LiFSI

(DME/HFE = 3:5 by volume), and the optimal ratio was selected by density functional theory (DFT) theoretical calculation and experimental combination. The electrolyte showed not only relatively good physical properties such as low viscosity and high conductivity but also decent electrochemical performance. The coulombic efficiency of Li||Cu half-batteries can remain at 99% or more even after circulating for 250 cycles under the conditions of 1 mA cm⁻² current density and 1 mAh cm⁻² lithium deposition amount every time, and the battery polarization voltage was stabilized at approximately 50 mV. In addition, based on this localized high-concentration electrolyte (LHCE), we added LiCO₂CF₃ for further improving the cathodic stability. The results showed that a 0.15 M lithium salt additive can significantly enhance the oxidation stability of the electrolyte, which allowed Li||NCM523 batteries to maintain about 83% capacity after cycling for 250 times with a 0.5 C charge current density and a 1 C discharge current density (1 C = 160 mAh g⁻¹) at a 4.3 V cutoff voltage. Of course, we also used it for half-cells testing. The results indicated that the introduction of the lithium salt additive had a little negative impact on the anode performance under the same condition as before, suggesting that this new kind of

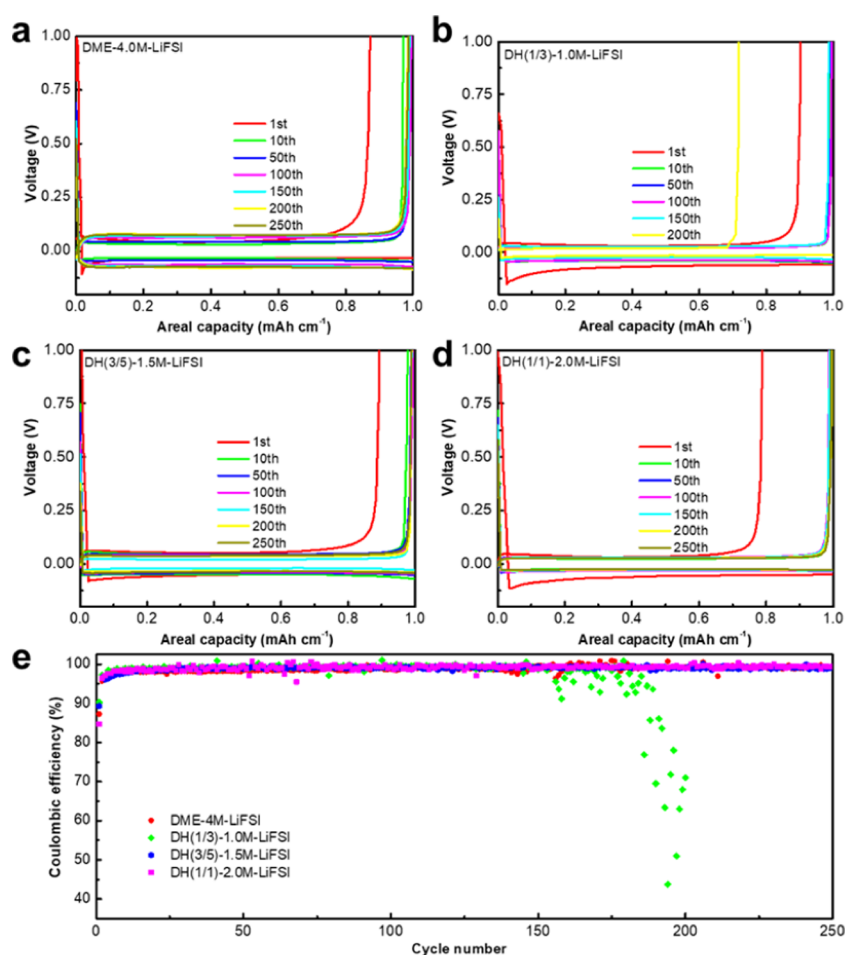


Figure 2. (a–d) Polarization voltage curves of LillCu half-cells under the conditions of 1 mA cm^{-2} current density and 1 mAh cm^{-2} lithium deposition with four electrolytes. (e) Cyclic performance of LillCu half-cells under four electrolyte conditions.

localized high-concentration electrolyte benefited both NCM523 cathode materials charged to a high voltage of 4.3 V and lithium-metal anode.

2. EXPERIMENTAL SECTION

2.1. Material Preparation. The active cathode material $\text{LiNi}_{0.5}\text{Co}_{0.2}\text{Mn}_{0.3}$ (NCM523), acetylene black (AB), and poly(vinylidene fluoride) (PVDF) binder were weighed at a weight ratio of 8:1:1 and ground to homogeneity. Then, they were stirred with 1-methyl-2-pyrrolidinone (NMP). After 6 h, the slurry was applied to aluminum (Al) foil. Before keeping it in an $80 \text{ }^\circ\text{C}$ vacuum oven for 12 h, it was placed on a hot plate at $50 \text{ }^\circ\text{C}$ for 30 min. The loading amount of the active cathode material was nearly 5 mg cm^{-2} . We added the HFE diluent into DME-4M-LiFSI to obtain a series of localized high-concentration ether electrolytes including DH(1/3)-1.0M-LiFSI, DH(3/5)-1.5M-LiFSI, and DH(1/1)-2.0M-LiFSI. Furthermore, DH(3/5)-1.65M-LiFC was acquired by adding 0.15 M LiCO_2CF_3 into DH(3/5)-1.5M-LiFSI. DME-based electrolytes were prepared by adding LiFSI into the DME solvent at different concentrations. LillCu half-cells and lithium-metal batteries were both in a 2016-type button. The pole piece and Li sheet are both 12 mm in diameter, and the electrolyte was added in 35 mL twice. The separator was provided by Celgard.

2.2. Material Characterization. Scanning electron microscopy (SEM) images were acquired by a field-emission scanning electron microscope (FESEM, HITACHI 4800); transmission electron microscopy (TEM) images were taken by a JEM2100 instrument; and X-ray photoelectron spectroscopy (XPS) data were obtained by the PHI Quantum 2000 test equipment. X-ray diffraction (XRD) data

were obtained on a Rigaku MiniFlex 600 X-ray diffractometer using Cu K2 as the target, with test angles ranging from 10 to 70° at a speed of 2° min^{-1} . ^{17}O NMR (nuclear magnetic resonance) spectra were recorded on an Ascend 600 MHz spectrometer at $25 \text{ }^\circ\text{C}$. Ionic conductivity and viscosity data were, respectively, tested by a DDS-307 conductivity meter and a SEKONIC 70A-ST viscometer at room temperature. Fourier transform infrared (FTIR) spectra were acquired on an infrared spectrometer (Thermo Fisher, IS5) under appropriate temperature and humidity.

2.3. Electrochemical Characterization. Linear sweep voltammetry (LSV) data were measured by a three-electrode system including an Al foil working electrode ($1.2 \times 1.2 \text{ cm}^2$) and lithium plates as the reference electrode/counter electrode on a CHI660B electrochemical workstation; The scanning rate was 1 mV s^{-1} . The LillCu half-cells and lithium-metal batteries were assembled in a Braun glovebox filled with an argon inert atmosphere, which had less than 0.1 ppm water oxygen content. The 2016-type button cells were assembled with copper foil or active material electrode, Celgard separator, and 1 mm thick lithium sheet simultaneously with a $2 \times 35 \mu\text{L}$ electrolyte. The galvanostatic charging and discharging data were measured at a constant temperature of $25 \text{ }^\circ\text{C}$ on the Land BT2000 test system.

3. RESULTS AND DISCUSSION

First, three localized high-concentration electrolytes (LHCEs) were obtained by adding different volumes of the diluent HFE to the DME-4M-LiFSI high-concentration electrolyte (HCE), and then the relevant physical and electrochemical properties were tested. It can be seen from Figure 1a that the viscosity of

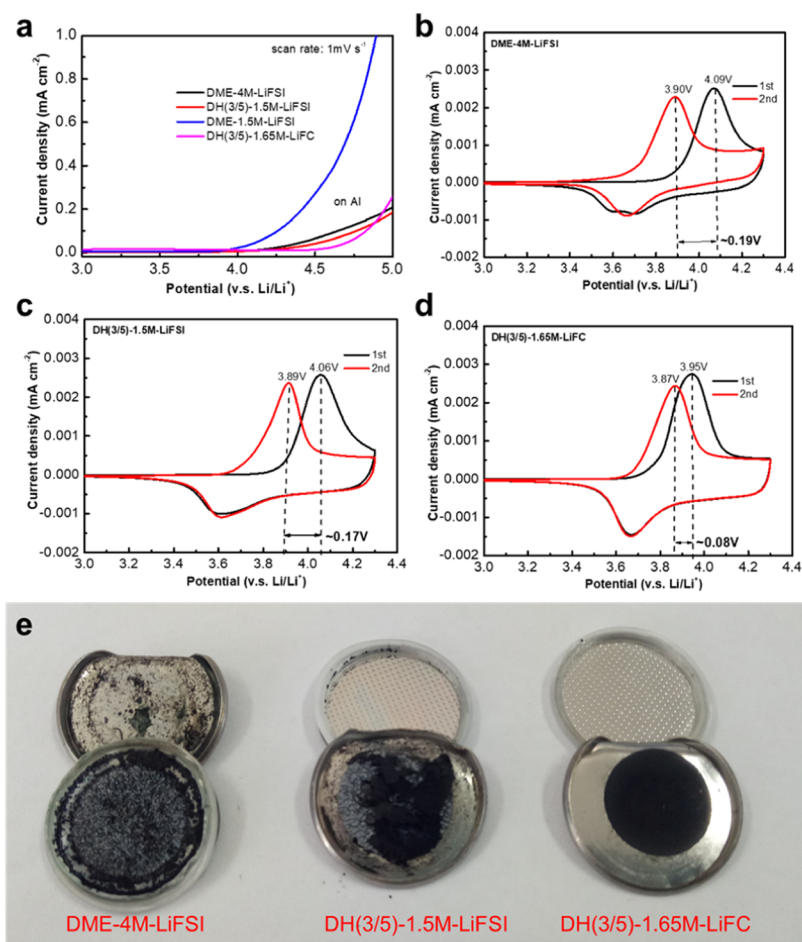


Figure 3. (a) LSV comparison results of four electrolytes on Al foil with a scan rate of 1 mV s⁻¹. (b–d) Cyclic voltammetry (CV) results of LillNCM523 batteries with a sweep speed of 0.5 mV s⁻¹ and voltage range of 3–4.3 V under three electrolyte conditions, respectively. (e) Cathode morphology comparison of LillNCM523 coin batteries in three kinds of electrolytes after 10 cycles under the conditions of a scanning speed of 0.5 mV s⁻¹ and a voltage range of 3–4.3 V.

LHCEs was significantly reduced and the ionic conductivity had been improved to some extent after adding the diluent. Especially, the ionic conductivity of DH(3/5)-1.5M-LiFSI (12.7 mS cm⁻¹) is much higher than 2.44 mS cm⁻¹ of the similar electrolyte reported by Ren et al.,⁴⁰ which may be due to the relatively higher content of DME and lower content of HFE under the same concentration. As we know, Li⁺ is usually accompanied with three to four solvent molecules in the dilute electrolyte, which is dominated with solvent-separated ion pairs (SSIPs) and free solvent molecules, while in the concentrated electrolyte, the number of solvent molecules coordinated with Li⁺ is reduced to one to two so that salt anions enter the solvation sheath to form contact ion pairs (CIPs) and cation–anion aggregates (AGGs).⁴¹ According to the ¹⁷O NMR characterization results of different electrolytes at 25 °C (Figure 1b), we can find that the chemical shifts of HCE and LHCEs have both widened compared to the dilute electrolytes, which means that both of them have similar aggregation states of CIPs and AGGs. On the other hand, compared to the HCE, the chemical shifts of the LHCEs had shifted slightly to the high field, and their peak shape in the vicinity of 170 cm⁻¹ became sharper, reflecting that the diluent HFE damaged the hinge structure in the solution to a certain extent, but with an increasing content of the diluent, the state of aggregation in the HCE was still maintained. And the whole

chemical shift all increased, indicating that their electron cloud density on the solvent oxygen had decreased, namely, the interaction between solvent and lithium salt was weakened, which was also consistent with the test results of ionic conductivity. In addition, we have also conducted a molecular dynamics (MD) simulation (Figure 1d) to simulate different coordination states with different electrolytes. As shown in Figure 1e, dilute electrolytes are dominated by the coordination number of 0, which means that they are mainly composed of SSIPs. However, when the concentration is increased to 4 M, its coordination numbers are mostly 1 and 2, indicating that CIPs and AGGs are dominant. Furthermore, the coordination numbers of LHCEs are closer to that of HCE and significantly different from that of low-concentration solution of the same concentration (more computational details can be found in the Supporting Information). As a result, the above phenomena experimentally and theoretically support our view that the addition of diluent can still make the electrolyte maintain some states of HCE and possess its characteristics.

Then, the above four electrolytes were used to test the electrochemical performance of LillCu half-cells. As shown in Figure 2: (1) Compared to the HCE, the battery polarization voltage under the LHCE condition was not significantly affected by the addition of dilute HFE, but when its content is

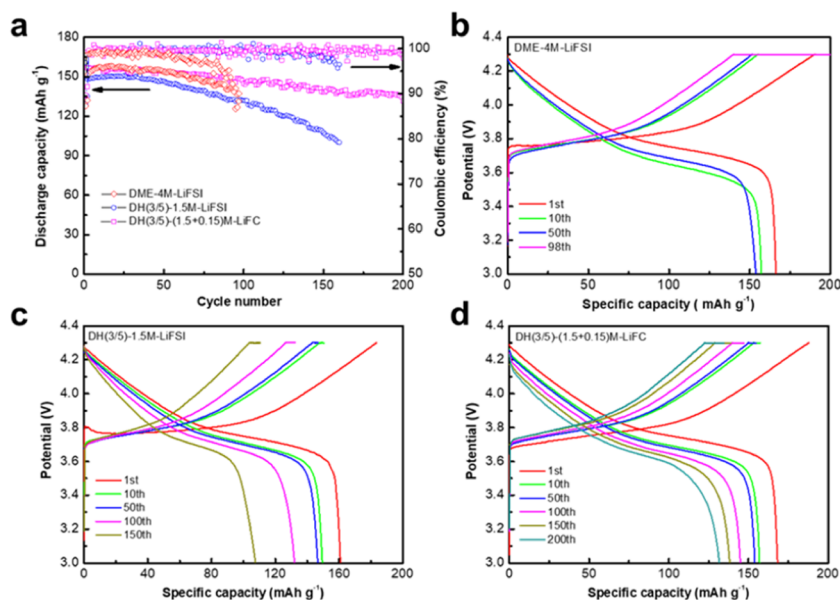


Figure 4. Cycle performance (a) and voltage–specific capacity curves (b–d) for a given number of cycles of LillNCMS23 batteries with a 0.5 C charge current density, a 1C discharge current density ($1\text{ C} = 160\text{ mA g}^{-1}$), and a 3–4.3 V voltage range with three electrolytes of DME-4M-LiFSI, DH(3/5)-1.5M-LiFSI, and DH(3/5)-1.65M-LiFC.

too high, the cyclic stability was still reduced, for example, DH(1/3)-1.0M-LiFSI showed obvious degradation; (2) among the three kinds of LHCEs, DH(3/5)-1.5M-LiFSI outstood to obtain relatively excellent electrochemical performance along with decent physical properties, that is, its coulombic efficiency remained higher than 99% after 250 cycles under the current density of 1 mA cm^{-2} and lithium deposition of 1 mAh cm^{-2} for each cycle, and the stable battery polarization voltage was also about 50 mV, comparable to that of the original HCE (DME-4M-LiFSI).

LSV tests were conducted to compare the electrochemical windows of different electrolytes, and the results can be seen in Figure 3a. We can find that DME-1.5M-LiFSI has a very limited antioxidant voltage (about 3.7 V) because of its inherent defect, while DH(3/5)-1.5M-LiFSI, a locally diluted solution of the same concentration, showed significantly improved oxidation stability and even had an oxidation potential of nearly 4.3 V, which was also much higher than that of HCE (DME-4M-LiFSI). Moreover, the antioxidant ability of DH(3/5)-1.65M-LiFC was further improved by adding a LiCO_2CF_3 lithium salt additive, providing a possibility for us to apply it to the high-voltage system. Based on the above phenomena, we performed Fourier transform infrared (FTIR) spectroscopy of pure solvents DME, lithium salt LiFSI, and four kinds of electrolytes to further investigate the intermolecular interactions between DME and LiFSI with different concentrations (shown in Figure S2a). It can be seen that as the electrolyte concentration increased, the characteristic peak of C–O–C of 1130 displayed a red shift gradually. DH(3/5)-1.5M-LiFSI and HCE had similar infrared absorption vibration peaks. And with the lithium salt additive LiCO_2CF_3 , DH(3/5)-1.65M-LiFC not only shifted to a lower wavenumber at 1107 cm^{-1} but also became broader, reflecting the stronger complexation between the lithium salt and the solvent. Due to complexation with Li^+ of lithium salts, the DME oxygen donates lone pairs to Li^+ , resulting in the reduction of the highest occupied molecular orbital (HOMO) energy level of DME,⁴² which is also

consistent with the results of LSV. The schematic representation of the interfacial stability of cathode enabled by the lower HOMO of DME-LiFSI-HFE- LiCO_2CF_3 and CEI is shown in Figure S2b.

In addition, the CV tests of LillNCMS23 batteries at a sweep speed of 0.5 mV s^{-1} and voltage range of 3–4.3 V with different electrolytes were performed. According to the CV characterization results (Figure 3b–d), it can be seen that the oxidation potentials of batteries in the initial cycle with the three electrolytes were 4.09, 4.06, and 3.95 V, respectively. And in the second cycle, they all had a similar and normal curve. The differences in the first two cycles indicated that the batteries were in different states and DH(3/5)-1.65M-LiFC enabled it to possess the best stability. We believe the reason for this phenomenon may be that the different stability of the electrolyte leads to different degrees of decomposition during the charging and discharging processes, resulting in the difference of electrode interface and thus affecting the normal electrochemical reaction of the electrode materials. On the other hand, we made a contrast of the cathode sheets cycled after 10 cycles in different electrolytes under the same conditions (as shown in Figure 3e), and it was obvious that except DH(3/5)-1.65M-LiFC, the LHCE with lithium salt additive kept the positive electrode plate intact after recycling and the other two kinds of electrolytes made the cathode plates powder obviously. We presume that this result is a reflection of the oxidation resistance of the electrolyte itself, and these phenomena also intuitively prove that the electrolyte we designed and optimized has obvious advantages in high-voltage systems.

Of course, galvanostatic test experiments of LillNCMS23 batteries were also conducted. In the first place, we charged the batteries at a relatively low current density of 0.1 C and then increased the charge current density to 0.5 C with a high discharge current density of 1 C. As can be seen from the results in Figure 4, the capacity of the batteries under HCE condition began to decline around 50 cycles, followed by overcharging. At the same time, DH(3/5)-1.5M-LiFSI

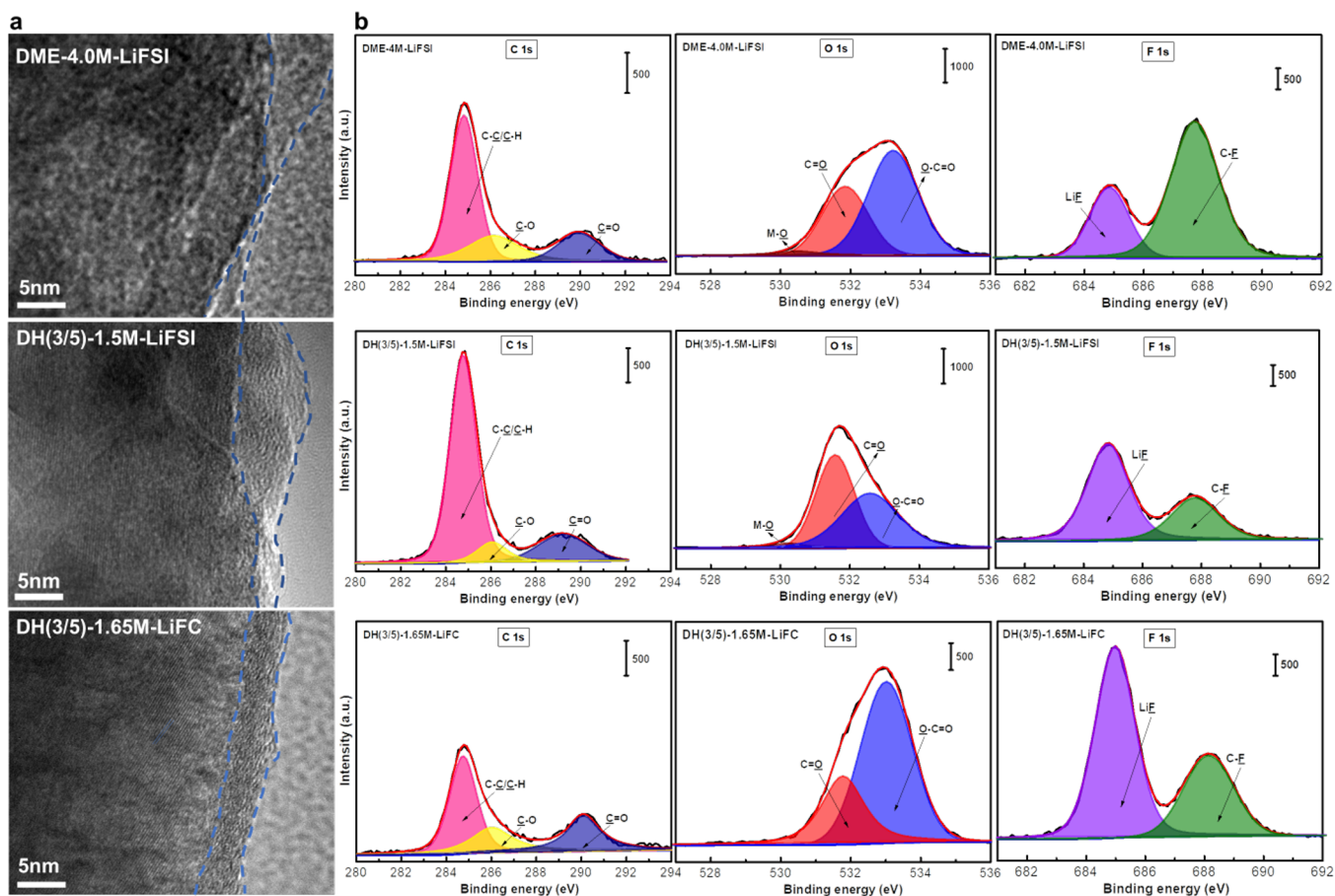


Figure 5. TEM (a) and XPS (b) characterization results of LillNCM523 cathode materials after 10 cycles in three electrolytes including DME-4M-LiFSI, DH(3/5)-1.5M-LiFSI, and DH(3/5)-1.65M-LiFC.

significantly improved the battery stability, and the batteries started overcharging in about 150 cycles. Meanwhile, DH(3/5)-1.65M-LiFC, the LHCE with lithium salt additive, could maintain the residual capacity of 83% in about 200 cycles, and there was no overcharging. The above results showed that LHCE modified with LiCO_2CF_3 lithium salt additive had obvious high-voltage oxidation stability, which also indicated that the lithium salt additive has great potential in positive electrode modification. And to ensure whether it had side effects on lithium-metal anode, performance tests of LillCu half-cells were also conducted (see Figure S1). To our surprise, under the same depositing/stripping condition as before for 250 cycles, the battery cycle performance and the polarization voltage changed almost equally before adding additive, which also suggested that it was a very promising multifunctional additive.

To further understand how the electrolyte functioned on the cathode side, TEM and XPS characterization tests (Figure 5) were carried out. First, we compared the TEM results of Lill NCM523 battery cathode sheets after 10 cycles in different electrolytes (Figure 5a), from which it can be found that cathode surface passivation films were generated with HCE and LHCE electrolytes, but their compactness and uniformity were quite poor, which was unfavorable for maintaining battery cycle stability. Meanwhile, using DH(3/5)-1.65M-LiFC, the cathode electrolyte interface (CEI) layer was obviously different from those with the other two electrolytes, which was very uniform with about 5 nm thickness. Furthermore, the

XPS data of C 1s, O 1s, and F 1s on the cathode surface after circulation (Figure 5b) showed that the passivation film components mostly included lithium fluoride (LiF), Li_2CO_3 , and lithium alkoxide (LiOR). Nevertheless, if no lithium salt additive was added, the components generated by solvent decomposition accounted for a large percentage. While adding the additive LiCO_2CF_3 for modifying, the solvent decomposition components obviously reduced, indicating that the addition of lithium salt did significantly inhibit the decomposition of electrolyte. In addition, a small amount of M–O (O 1s, 530 eV) in the cathode surface using the two electrolytes without additive was also observed, suggesting that the cathode material partially dissolved during the cycling process and thus led to fast capacity decay of batteries, which also corresponded with the electrochemical performance. On the other hand, after HFE was added, the content of LiF in the CEI layer component increased slightly, indicating its role as a high-voltage additive, and also had a certain role in inhibiting the dissolution of positive materials. Of course, to optimize the performance, it needs to combine HFE with LiCO_2CF_3 at the same time.

Besides, the mechanism of electrolyte in lithium-metal negative electrode was further revealed by conducting SEM and XPS characterization tests. From the SEM characterization results in Figure 6, we can see that the surface states of lithium metal were all similar to the “nodule-like structure with round-shaped edges”²⁹ without too much change after LillCu half-cells circulated for 50 times in three electrolytes. While under

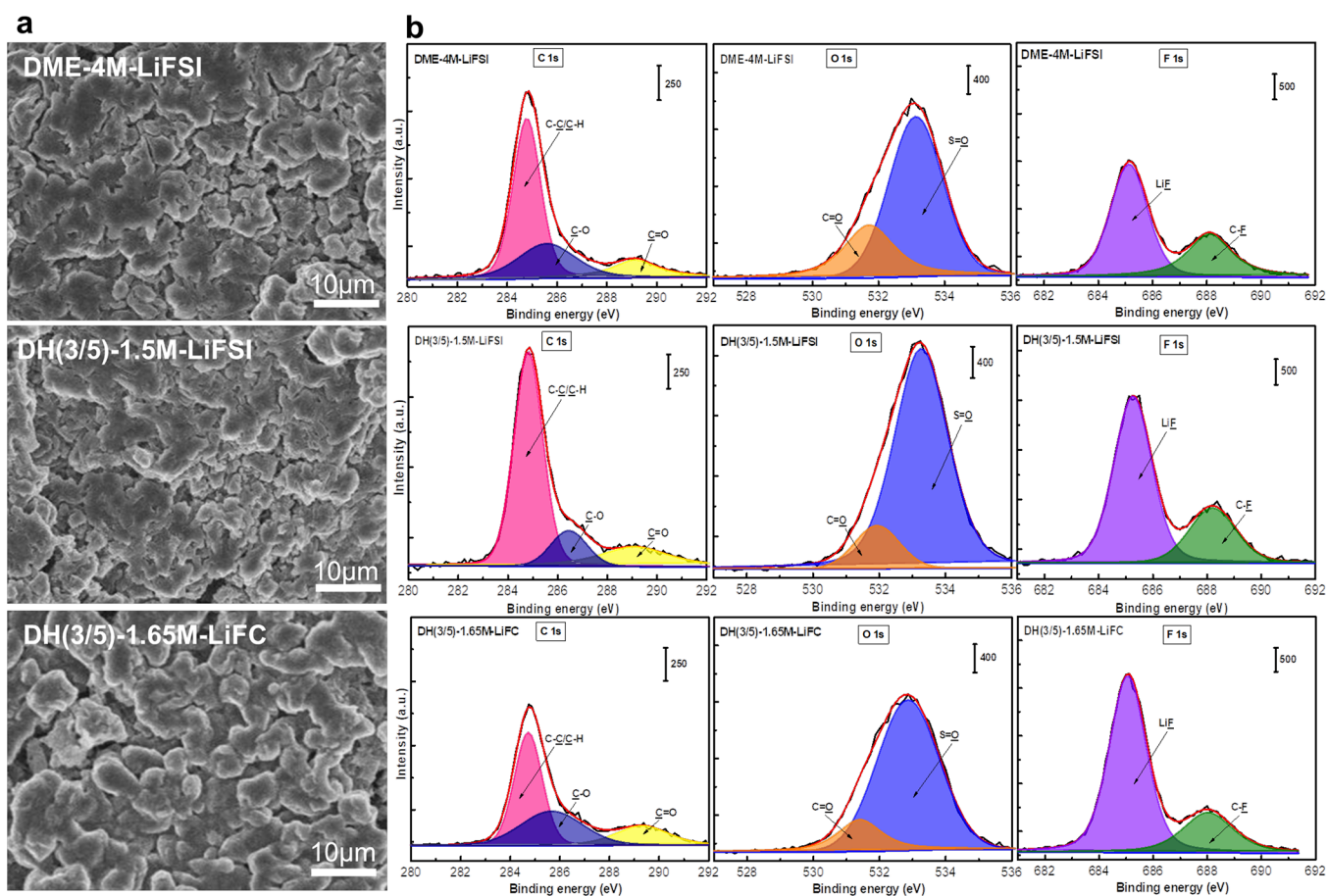


Figure 6. Characterization results of SEM (a) and XPS (b) on the 50-times cycled Li metal surface of LillCu half-cells with three electrolytes including DME-4M-LiFSI, DH(3/5)-1.5M-LiFSI, and DH(3/5)-1.65M-LiFC.

the condition of LHCEs, the components of LiF were significantly improved, which should be mainly due to the addition of fluorine-containing ether. Meanwhile, we can see the XPS data of C 1s and O 1s in the LHCE with a 0.15 M additive, DH(3/5)-1.65M-LiFC, whose peak areas are relatively smaller than those of the other two electrolytes, which may suggest the decrease of Li_2CO_3 . Furthermore, the peak area of F 1s is also the biggest among the three electrolytes, which can be mostly attributed to the decomposition of both LiFSI and $\text{Li}_2\text{CO}_2\text{CF}_3$, and the reaction mechanism of $\text{Li}_2\text{CO}_2\text{CF}_3$ has been reported.⁴³ As a result, in terms of various components, the electrolyte before and after modification had no significant difference in maintaining the good performance of lithium-metal anode, which further indicated that LiCO_2CF_3 was beneficial to the improvement of battery performance.

4. CONCLUSIONS

We used the commonly used inert solvent HFE to dilute the DME-based concentrated ether electrolyte of 4 M LiFSI reported in the literature, and combined with theoretical calculation to optimize the ratio, we preliminarily determined that the electrolyte DH(3/5)-1.5M-LiFSI (DME/HFE = 3/5 by volume) had relatively good physical and electrochemical properties. This LHCE made LillCu half-cells still retain more than 99% of the coulombic efficiency under the current density of 1 mA cm^{-2} and lithium deposition amount for each cycle of 1 mAh cm^{-2} after 250 cycles, and the stable battery

polarization voltage was approximately 50 mV. Besides, this electrolyte with 0.15 M LiCO_2CF_3 further improved antioxidation and enabled LillNCMS23 batteries to achieve 83% capacity retention with a 0.5 C charge current density and a 1 C discharge current density ($1 \text{ C} = 160 \text{ mA g}^{-1}$) at a 4.3 V cutoff voltage after 250 cycles. Of course, the results of the Lill Cu half-cells also showed that the introduction of lithium salt additive had almost no negative impact on lithium anode performance, indicating that this new localized high-concentration DME-based electrolyte can not only stabilize the high-voltage cathode but also has good compatibility to lithium-metal anode.

■ ASSOCIATED CONTENT

Supporting Information

The Supporting Information is available free of charge at <https://pubs.acs.org/doi/10.1021/acsami.0c07904>.

Electrochemical performance of LillCu half-cells in the DH(3/5)-1.65M-LiFC electrolyte; FT-IR data of DME, LiFSI, and four kinds of electrolytes; HOMO and LUMO values of solvents and lithium salts in the electrolyte; and details of the theoretical calculation (PDF)

■ AUTHOR INFORMATION

Corresponding Author

Jinbao Zhao – State-Province Joint Engineering Laboratory of Power Source Technology for New Energy Vehicle, Engineering

Research Center of Electrochemical Technology, Ministry of Education, College of Chemistry and Chemical Engineering, Xiamen University, Xiamen 361005, P. R. China; orcid.org/0000-0002-2753-7508; Phone: +86-05922186935; Email: jbzhao@xmu.edu.cn

Authors

Shuangshuang Lin – State-Province Joint Engineering Laboratory of Power Source Technology for New Energy Vehicle, Engineering Research Center of Electrochemical Technology, Ministry of Education, College of Chemistry and Chemical Engineering, Xiamen University, Xiamen 361005, P. R. China

Haiming Hua – State-Province Joint Engineering Laboratory of Power Source Technology for New Energy Vehicle, Engineering Research Center of Electrochemical Technology, Ministry of Education, College of Chemistry and Chemical Engineering, Xiamen University, Xiamen 361005, P. R. China

Zhisen Li – State-Province Joint Engineering Laboratory of Power Source Technology for New Energy Vehicle, Engineering Research Center of Electrochemical Technology, Ministry of Education, College of Chemistry and Chemical Engineering, Xiamen University, Xiamen 361005, P. R. China

Complete contact information is available at: <https://pubs.acs.org/10.1021/acsami.0c07904>

Notes

The authors declare no competing financial interest.

ACKNOWLEDGMENTS

The authors greatly appreciate the financial support of National Natural Science Foundation of China (21875195), National Key Research and Development Program of China (2017YFB0102000), and the Fundamental Research Funds for the Central Universities (20720190040). They also thank Jing Zeng for her valuable advice on the draft.

REFERENCES

- (1) Fang, C.; Wang, X.; Meng, Y. Key Issues Hindering a Practical Lithium-Metal Anode. *Trends in Chemistry* **2019**, *1*, 152–158.
- (2) Wang, L.; Ma, J.; Wang, C.; Yu, X.; Liu, R.; Jiang, F.; Sun, X.; Du, A.; Zhou, X.; Cui, G. A Novel Bifunctional Self-Stabilized Strategy Enabling 4.6 V LiCoO₂ with Excellent Long-Term Cyclability and High-Rate Capability. *Adv. Sci.* **2019**, *6*, No. 1900355.
- (3) Winter, M.; Barnett, B.; Xu, K. Before Li Ion Batteries. *Chem. Rev.* **2018**, *118*, 11433–11456.
- (4) Wang, L.; Chen, B.; Ma, J.; Cui, G.; Chen, L. Reviving lithium cobalt oxide-based lithium secondary batteries-toward a higher energy density. *Chem. Soc. Rev.* **2018**, *47*, 6505–6602.
- (5) Goodenough, J. B.; Kim, Y. Challenges for Rechargeable Li Batteries. *Chem. Mater.* **2010**, *22*, 587–603.
- (6) Armand, M.; Tarascon, J. M. Building better batteries. *Nature* **2008**, *451*, 652–657.
- (7) Tarascon, J. M.; Armand, M. Issues and challenges facing rechargeable lithium batteries. *Nature* **2001**, *414*, 359–367.
- (8) Jo, M.; Jeong, S.; Cho, J. High power LiCoO₂ cathode materials with ultra energy density for Li-ion cells. *Electrochem. Commun.* **2010**, *12*, 992–995.
- (9) Sun, Y.; Zhao, Y.; Wang, J.; Liang, J.; Wang, C.; Sun, Q.; Lin, X.; Adair, K. R.; Luo, J.; Wang, D.; Li, R.; Cai, M.; Sham, T. K.; Sun, X. A Novel Organic “Polyurea” Thin Film for Ultralong-Life Lithium-Metal Anodes via Molecular-Layer Deposition. *Adv. Mater.* **2018**, *31*, No. 1806541.

(10) Shi, P.; Zhang, L.; Xiang, H.; Liang, X.; Sun, Y.; Xu, W. Lithium Difluorophosphate as a Dendrite-Suppressing Additive for Lithium Metal Batteries. *ACS Appl. Mater. Interfaces* **2018**, *10*, 22201–22209.

(11) Yan, C.; Yao, Y. X.; Chen, X.; Cheng, X. B.; Zhang, X. Q.; Huang, J. Q.; Zhang, Q. Lithium Nitrate Solvation Chemistry in Carbonate Electrolyte Sustains High-Voltage Lithium Metal Batteries. *Angew. Chem., Int. Ed.* **2018**, *57*, 14055–14059.

(12) Yan, C.; Cheng, X. B.; Tian, Y.; Chen, X.; Zhang, X. Q.; Li, W. J.; Huang, J. Q.; Zhang, Q. Dual-Layered Film Protected Lithium Metal Anode to Enable Dendrite-Free Lithium Deposition. *Adv. Mater.* **2018**, *30*, No. 1707629.

(13) Trinh, N. D.; Lepage, D.; Ayme-Perrot, D.; Badia, A.; Dolle, M.; Rochefort, D. An Artificial Lithium Protective Layer that Enables the Use of Acetonitrile-Based Electrolytes in Lithium Metal Batteries. *Angew. Chem., Int. Ed.* **2018**, *57*, 5072–5075.

(14) Liu, S.; Xia, X.; Deng, S.; Xie, D.; Yao, Z.; Zhang, L.; Zhang, S.; Wang, X.; Tu, J. In Situ Solid Electrolyte Interphase from Spray Quenching on Molten Li: A New Way to Construct High-Performance Lithium-Metal Anodes. *Adv. Mater.* **2018**, *31*, No. 1806470.

(15) Li, Y.; Yang, Z.; Wu, Z.; Li, J.; Zou, J.; Jiang, C.; Yang, J.; Wang, L.; Niu, X. The effects of lithium salt and solvent on lithium metal anode performance. *Solid State Ionics* **2018**, *324*, 144–149.

(16) Li, X.; Zheng, J.; Ren, X.; Engelhard, M. H.; Zhao, W.; Li, Q.; Zhang, J.-G.; Xu, W. Dendrite-Free and Performance-Enhanced Lithium Metal Batteries through Optimizing Solvent Compositions and Adding Combinational Additives. *Adv. Energy Mater.* **2018**, *8*, No. 1703022.

(17) Li, H.; Li, M.; Siyal, S. H.; Zhu, M.; Lan, J.-L.; Sui, G.; Yu, Y.; Zhong, W.; Yang, X. A sandwich structure polymer/polymer-ceramics/polymer gel electrolytes for the safe, stable cycling of lithium metal batteries. *J. Membr. Sci.* **2018**, *555*, 169–176.

(18) Kim, M. S.; Ryu, J.-H.; Deepika; Lim, Y. R.; Nah, I. W.; Lee, K.-R.; Archer, L. A.; Il Cho, W. Langmuir–Blodgett artificial solid-electrolyte interphases for practical lithium metal batteries. *Nat. Energy* **2018**, *3*, 889–898.

(19) Jiao, S.; Ren, X.; Cao, R.; Engelhard, M. H.; Liu, Y.; Hu, D.; Mei, D.; Zheng, J.; Zhao, W.; Li, Q.; Liu, N.; Adams, B. D.; Ma, C.; Liu, J.; Zhang, J.-G.; Xu, W. Stable cycling of high-voltage lithium metal batteries in ether electrolytes. *Nat. Energy* **2018**, *3*, 739–746.

(20) Zheng, J.; Engelhard, M. H.; Mei, D.; Jiao, S.; Polzin, B. J.; Zhang, J.-G.; Xu, W. Electrolyte additive enabled fast charging and stable cycling lithium metal batteries. *Nat. Energy* **2017**, *2*, No. 17012.

(21) Xu, X.; Liu, J.; Liu, Z.; Shen, J.; Hu, R.; Liu, J.; Ouyang, L.; Zhang, L.; Zhu, M. Robust Pitaya-Structured Pyrite as High Energy Density Cathode for High-Rate Lithium Batteries. *ACS Nano* **2017**, *11*, 9033–9040.

(22) Wood, K. N.; Noked, M.; Dasgupta, N. P. Lithium Metal Anodes: Toward an Improved Understanding of Coupled Morphological, Electrochemical, and Mechanical Behavior. *ACS Energy Lett.* **2017**, *2*, 664–672.

(23) Lu, Q.; He, Y. B.; Yu, Q.; Li, B.; Kaneti, Y. V.; Yao, Y.; Kang, F.; Yang, Q. H. Dendrite-Free, High-Rate, Long-Life Lithium Metal Batteries with a 3D Cross-Linked Network Polymer Electrolyte. *Adv. Mater.* **2017**, *29*, No. 1604460.

(24) Liu, Y.; Lin, D.; Yuen, P. Y.; Liu, K.; Xie, J.; Dauskardt, R. H.; Cui, Y. An Artificial Solid Electrolyte Interphase with High Li-Ion Conductivity, Mechanical Strength, and Flexibility for Stable Lithium Metal Anodes. *Adv. Mater.* **2017**, *29*, No. 1605531.

(25) Alvarado, J.; Schroeder, M. A.; Pollard, T. P.; Wang, X.; Lee, J. Z.; Zhang, M.; Wynn, T.; Ding, M.; Borodin, O.; Meng, Y. S.; Xu, K. Bisalt ether electrolytes: a pathway towards lithium metal batteries with Ni-rich cathodes. *Energy & Environ. Sci.* **2019**, *12*, 780–794.

(26) Pranay Reddy, K.; Fischer, P.; Marinaro, M.; Wohlfahrt-Mehrens, M. Improved Li-Metal Cycling Performance in High Concentrated Electrolytes for Li-O₂ Batteries. *Chem. Electro. Chem.* **2018**, *5*, 2758–2766.

(27) Fan, X.; Chen, L.; Ji, X.; Deng, T.; Hou, S.; Chen, J.; Zheng, J.; Wang, F.; Jiang, J.; Xu, K.; Wang, C. Highly Fluorinated Interphases Enable High-Voltage Li-Metal Batteries. *Chem.* **2018**, *4*, 174–185.

(28) Zheng, J.; Yan, P.; Mei, D.; Engelhard, M. H.; Cartmell, S. S.; Polzin, B. J.; Wang, C.; Zhang, J.-G.; Xu, W. Highly Stable Operation of Lithium Metal Batteries Enabled by the Formation of a Transient High-Concentration Electrolyte Layer. *Adv. Energy Mater.* **2016**, *6*, No. 1502151.

(29) Qian, J.; Henderson, W. A.; Xu, W.; Bhattacharya, P.; Engelhard, M.; Borodin, O.; Zhang, J. G. High rate and stable cycling of lithium metal anode. *Nat. Commun.* **2015**, *6*, 6362–6370.

(30) Li, L.; Basu, S.; Wang, Y.; Chen, Z.; Hundekar, P.; Wang, B.; Shi, J.; Shi, Y.; Narayanan, S.; Koratkar, N. Self-heating–induced healing of lithium dendrites. *Science* **2018**, *359*, 1513–1516.

(31) Jeong, S.-K.; Seo, H.-Y.; Kim, D.-H.; Han, H.-K.; Kim, J.-G.; Lee, Y. B.; Iriyama, Y.; Abe, T.; Ogumi, Z. Suppression of dendritic lithium formation by using concentrated electrolyte solutions. *Electrochem. Commun.* **2008**, *10*, 635–638.

(32) Suo, L.; Hu, Y. S.; Li, H.; Armand, M.; Chen, L. A new class of Solvent-in-Salt electrolyte for high-energy rechargeable metallic lithium batteries. *Nat. Commun.* **2013**, *4*, No. 1481.

(33) Matsumoto, K.; Inoue, K.; Nakahara, K.; Yuge, R.; Noguchi, T.; Utsugi, K. Suppression of aluminum corrosion by using high concentration LiTFSI electrolyte. *J. Power Sources* **2013**, *231*, 234–238.

(34) Yoon, H.; C. H, P.; Best, A. S.; Forsyth, M.; MacFarlane, D. R. Fast charge/discharge of Li metal batteries using an ionic liquid electrolyte. *J. Electrochem. Soc.* **2013**, *160*, A1629.

(35) Zhang, S. S.; Xu, K.; Jow, T. R. Enhanced performance of Li-ion cell with LiBF₄-PC based electrolyte by addition of small amount of LiBOB. *J. Power Sources* **2006**, *156*, 629–633.

(36) Ren, X.; Chen, S.; Lee, H.; Mei, D.; Engelhard, M. H.; Burton, S. D.; Zhao, W.; Zheng, J.; Li, Q.; Ding, M. S.; Schroeder, M.; Alvarado, J.; Xu, K.; Meng, Y. S.; Liu, J.; Zhang, J.-G.; Xu, W. Localized High-Concentration Sulfone Electrolytes for High-Efficiency Lithium-Metal Batteries. *Chem.* **2018**, *4*, 1877–1892.

(37) Zheng, J.; Ji, G.; Fan, X.; Chen, J.; Li, Q.; Wang, H.; Yang, Y.; DeMella, K. C.; Raghavan, S. R.; Wang, C. High-Fluorinated Electrolytes for Li–S Batteries. *Adv. Energy Mater.* **2019**, *9*, No. 1803774.

(38) Chen, S.; Zheng, J.; Mei, D.; Han, K. S.; Engelhard, M. H.; Zhao, W.; Xu, W.; Liu, J.; Zhang, J. G. High-Voltage Lithium-Metal Batteries Enabled by Localized High-Concentration Electrolytes. *Adv. Mater.* **2018**, *30*, No. 1706102.

(39) Yu, L.; Chen, S.; Lee, H.; Zhang, L.; Engelhard, M. H.; Li, Q.; Jiao, S.; Liu, J.; Xu, W.; Zhang, J.-G. A Localized High-Concentration Electrolyte with Optimized Solvents and Lithium Difluoro(oxalate)-borate Additive for Stable Lithium Metal Batteries. *ACS Energy Lett.* **2018**, *3*, 2059–2067.

(40) Ren, X.; Zou, L.; Cao, X.; Engelhard, M. H.; Liu, W.; Burton, S. D.; Lee, H.; Niu, C.; Matthews, B. E.; Zhu, Z.; Wang, C.; Arey, B. W.; Xiao, J.; Liu, J.; Zhang, J.-G.; Xu, W. Enabling High-Voltage Lithium-Metal Batteries under Practical Conditions. *Joule* **2019**, *3*, 1662–1676.

(41) Zheng, J.; Lochala, J. A.; Kwok, A.; Deng, Z. D.; Xiao, J. Research Progress towards Understanding the Unique Interfaces between Concentrated Electrolytes and Electrodes for Energy Storage Applications. *Adv. Sci.* **2017**, *4*, No. 1700032.

(42) Wang, C.; W, T.; Wang, L.; Hu, Z.; Cui, Z.; Li, J.; Dong, S.; Zhou, X.; Cui, G. Differentiated Lithium Salt Design for Multilayered PEO Electrolyte Enables a High-Voltage Solid-State Lithium Metal Battery. *Adv. Sci.* **2019**, *6*, No. 1901036.

(43) Wang, Z.; Qi, F.; Yin, L.; Shi, Y.; Sun, C.; An, B.; Cheng, H. M.; Li, F. An Anion-Tuned Solid Electrolyte Interphase with Fast Ion Transfer Kinetics for Stable Lithium Anodes. *Adv. Energy Mater.* **2020**, *10*, No. 1903843.